Solid state solar cell made from nanocrystalline TiO_2 with a fluorene-thiophene copolymer as a hole-conductor

P. Ravirajan[1, 2], S. A. Haque[3], D. Poplavskyy[1], J. R. Durrant[3],
D. D. C. Bradley[1] and J. Nelson[1]

[1]Centre for Electronic Materials and Devices, Dept. of Physics, Imperial College London, Prince Consort Road, London SW7 2BW, U.K;

[2]Dept. of Physics, University of Jaffna, Jaffna, Sri Lanka;

[3]Centre for Electronic Materials and Devices, Dept. of Chemistry, Imperial College London, Exhibition Road, London SW7 2AZ, U.K.

ABSTRACT

We study the charge recombination kinetics and photovoltaic performance of composites of poly (9,9-dioctylfluorene-co-bithiophene) polymer with nanocrystalline TiO_2. Transient optical spectroscopy confirms that photoexciation of the polymer leads to electron transfer to the TiO_2 and indicates that charge recombination is slow with a half-life of 100μs to 10ms. Polymer penetration into thick porous TiO_2 layers is improved by melt-processing and treatment of the TiO_2 surface. We study the photovoltaic characteristics of devices with different layer thickness and interface morphology. Quantum efficiency (QE) of all devices is increased by reducing the TiO_2 and polymer layer thickness. Inserting a thin porous TiO_2 layer in to a thin bi-layer device increases the QE by a factor of five. The improved device shows peak QE and monochromatic power conversion efficiencies of over 11% and 1% at 440nm respectively. The device produced a short-circuit current density of 300μAcm^{-2}, a fill factor of 0.24 and an open-circuit voltage of 0.8V under AM1.5 illumination. The fill factor is increased from 0.24 to 0.40 by introducing an additional dip-coating layer and overall power conversion efficiency is increased by 50 %. However, the device produced degraded current-voltage characteristics. We investigate this using an alternative polymers and different top contact metals.

Keywords: Solar cells, Polymer, Nanocrystalline TiO_2

1. INTRODUCTION

In recent years, there has been heightened interest in organic solar cells on account of their range of potential applications, their ease of fabrication and low cost compared to inorganic solar cells[1-5]. Although power efficiencies of 10 % have been reported for liquid electrolyte dye sensitized TiO_2 solar cells[6], there are a number of disadvantages, such as the requirement for complex encapsulation of the device and the chemically aggressive redox system, which limit the cell's practical applications. These disadvantages prompted the search for solid state alternatives. There have been several approaches for solid state organic based solar cells[7-12]. One of the approaches is to replace the electrolyte in a dye sensitised solar cell with a hole conducting polymer. Another promising approach is to replace both dye and liquid electrolyte with a hole conducting polymer which acts as both light absorber and hole-conductor resulting in hybrid solar cells.

The capability of conjugated polymers to sensitize TiO_2 to visible light, has been reported for various polymers such as MEH-PPV[13-18], PA-PPV[19], MDMO-PPV[20], and poly alkyl thiophenes[21-23]. MEH-PPV and TiO_2 is one of the best studied material combinations for TiO_2/polymer solar cells and its peak quantum efficiencies of about 10 %

Organic Photovoltaics IV, edited by Zakya H. Kafafi, Paul A. Lane, Proceedings of SPIE
Vol. 5215 (SPIE, Bellingham, WA, 2004) · 0277-786X/04/$15 · doi: 10.1117/12.506017

at 500 nm have been reported [16]. In such systems, performance is limited by the poor hole-mobility of the MEH-PPV polymer and limited interfacial area for charge separation between TiO_2 and polymer layers. Use of a high hole-mobility polymer should improve device performance.

In this study, we focus on a system consisting of a high hole mobility poly (9,9-dioctylfluorene-co-bithiophene) (F8T2) polymer[24] in contact with TiO_2 substrates of different morphology. This polymer possesses a liquid crystal phase at 260^0C[25]. We show that polymer penetration into porous films can be achieved either by melt processing and chemical treatment of the TiO_2 surface in thick TiO_2 film devices or by using a dip coating step. We find that device performance is limited by device thickness, interface morphology, top contact and interfacial energy step at the polymer/metal interface.

2. EXPERIMENTAL

2.1 Materials

Two hole-conducting polymers have been used in this study, poly(9,9-dioctylfluorene-co-bithiophene)(F8T2) and poly(9,9-dioctylfluorene-*co*-bis-*N*,*N*'-(4-butylphenyl)-bis-*N*,*N*'-phenyl-1,4-phenylenediamine)(PFB). Their chemical structures are shown in Figure 1. These polymers were dissolved in toluene at concentrations of 10-20 mg/ml. Colloidal TiO_2 paste (~15nm diameter, 50 % porosity) was prepared by a sol-gel route as described in ref. [26].

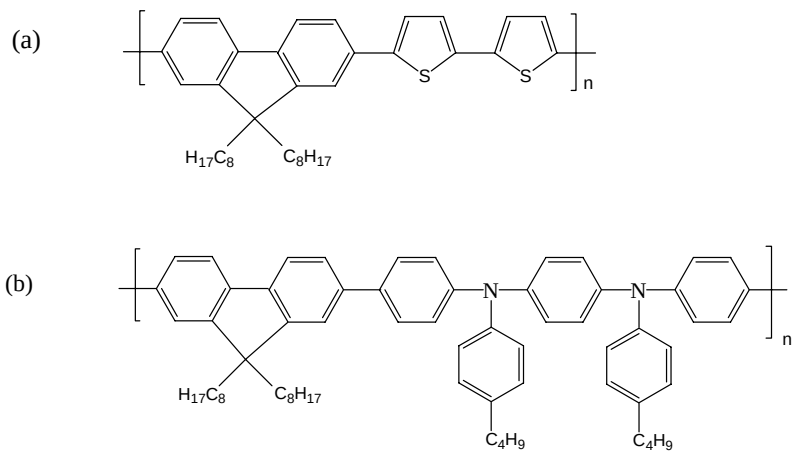

Figure 1. Chemical structures of (a) Poly(9,9-dioctylfluorene-co-bithiophene) (F8T2) and (b) Poly (9,9-dioctylfluorene-*co*-bis-*N*,*N*'-(4-butyl phenyl)-bis-*N*,*N*'-phenyl-1,4-phenylenediamine) (PFB).

2.2 Sample fabrication

All samples were prepared on Indium Tin Oxide (ITO) coated glass substrates (~1 cm^2), which were first cleaned by ultrasonic agitation in acetone and isopropanol. The cleaned substrate was then covered with a dense TiO_2 layer using a spray pyrolysis technique[27]. This dense layer prevents direct contact between the polymer and the substrate and is called the 'Hole Blocking Layer' (HBL). For 'thick' multi-layer samples, a 500-1000 nm layer of porous TiO_2 was deposited by doctor blading a colloidal paste in carbowax on to the HBL. For 'thin' multi-layer samples, a thin porous TiO_2 layer of thickness about 100 nm was deposited by spin coating (2000 rpm) a diluted aqueous colloidal paste on to the HBL. The layers were then sintered at 450^0C for 30 minutes. The hole-conductor was applied by spin coating a solution of polymer in toluene (10-20mg/ml) at 1000-2000 rpm, which produced a polymer layer thickness of 50-200 nm. For bi-layer samples, the polymer was spin coated directly on to the HBL. The thickness of all the films was measured using a Tencor Alpha-Step 200 profilometer. For electrical measurements, gold or aluminium contacts were deposited onto the polymer film by evaporation though a shadow mask. Each sample contained six devices of active area of about 0.045 cm^2.

2.3 Electrical measurements

The sample was housed in a home built sample holder with a quartz window for electrical measurements. All measurements were taken under vacuum. The light source was a 100 W xenon lamp, which was driven by a Bentham 505 stabilized power supply. The light from the lamp was dispersed by a CM110, 1/8m monochromator. Current and voltage (I-V) measurements were taken using a computer controlled Keithley 237 high voltage SMU (source measure unit).

For quantum efficiency (QE) measurements, the photocurrent of the sample, and the photocurrent of a calibrated silicon photodiode were obtained at a particular position for different wavelengths. The intensity of the light was calculated as a function of wavelength using the spectral response and photocurrent spectra of the silicon photodiode held at the same position as the sample. Monochromatic I-V curves were taken at the wavelength which gave the highest photocurrent. The I-V characteristic in the dark was measured before and after the illuminated I-V characteristic in order to confirm that the device behaviour had not changed. I-V characteristics were also measured under simulated sunlight using a home built potentiostat measurement unit with computer control and a halogen lamp calibrated to air mass (AM) 1.5 equivalent intensity (100 mW cm^{-2}).

2.4 Optical measurements

Uncontacted samples on ITO substrates were used for optical measurements. Photoinduced charge transfer yield and recombination kinetics were measured using nanosecond–millisecond transient optical spectroscopy as described in ref [28]. For F8T2/TiO_2 samples, the pump wavelength was 500 nm and the probe wavelength 720 nm. The transient optical spectrum, which peaks at about 720 nm, was assigned to the positive polaron in F8T2 after comparison with the absorption spectrum of the chemically oxidized polymer. The decay in absorbance as a function of time after the laser pulse is attributed to recombination of F8T2 polarons with electrons in TiO_2.

3. RESULTS

3.1 Effect of top electrode

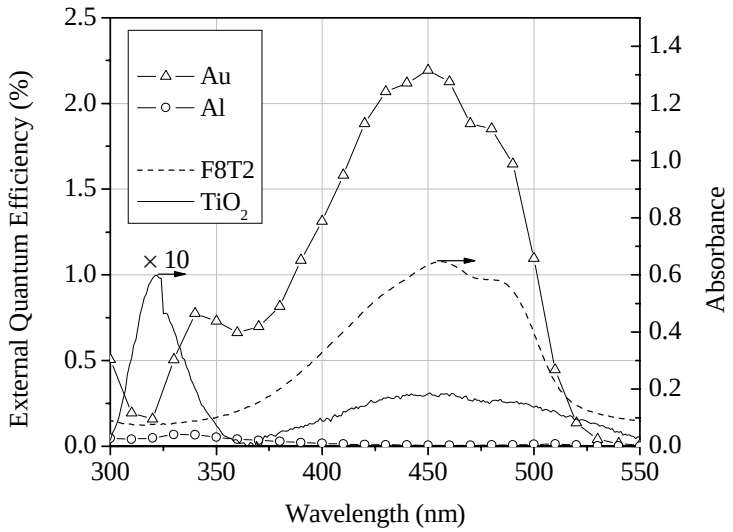

Figure 2. External quantum efficiency spectra of ITO/HBL(50nm)/F8T2(50nm)/metal bi-layer devices. Absorption spectra of F8T2 polymer film of thickness 50 nm on ITO (dashed line) and dense TiO_2 of thickness 50 nm on ITO (solid line) are also shown for comparison. The absorption spectrum of TiO_2 has been multiplied by a factor of ten.

Figure 2 shows a comparison of external quantum efficiency spectra for ITO/HBL(50nm)/F8T2(50nm)/metal bi-layer devices with different top electrodes. The optical absorption spectra of the dense 50 nm TiO_2 layer and 50 nm

polymer layer are included on the same Figure. Comparison between the absorption spectra and quantum efficiency spectra shows that the photocurrent is predominantly due to absorption in the polymer for the device with the Au electrode and due to absorption in TiO_2 in the device with the Al electrode. The Au device generates a photocurrent directed from ITO to Au, with a maximum quantum efficiency of about 1.3 %, while the device with Al electrode generates a negative photocurrent with quantum efficiency two orders of magnitude smaller. In the first case, the high work function of Au (nominally 5.1 eV) compared to that of ITO (4.5 eV, measured by Kelvin probe measurement) establishes an electrostatic driving force attracting holes to the metal and electrons to the ITO. In the case of the Al contact (work function ~4.3 eV) the polarity is reversed and electrons are drawn through the polymer. The very low QE in this case indicates that TiO_2 is a poor hole-conductor and/or that the polymer is a poor electron conductor. We conclude that a high work function cathode is needed to collect photocurrent in this system. Note that this is the reverse to most organic solar cell structures, where holes travel to the ITO and a low work function top contact is needed to collect electrons. Studies of Pt contacted devices further support our conclusion[29].

3.2 Effect of surface and heat treatment

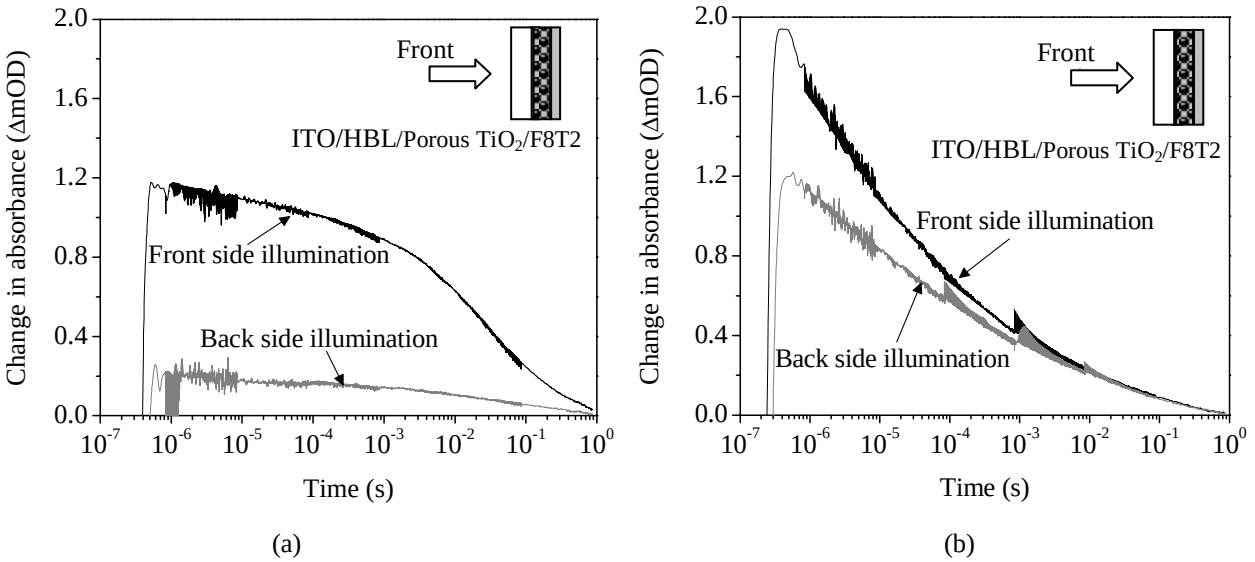

Figure 3. Transient absorption signals for (a) untreated and (b) treated samples of structure ITO/HBL(100 nm)/Porous TiO_2(600 nm)/F8T2(200 nm). The inserts show the device structure. The transient absorption signal is due to the positive polaron state of the F8T2 polymer at 720 nm following laser pulse excitation at 500 nm, at an excitation density of 50 μJ/pulse/cm^2. The decay is assigned to recombination between electrons in TiO_2 and $F8T2^+$ polarons. Black curves represent transient absorption kinetics for front side illumination, while grey curves represent back side illumination. The difference between the response for front (TiO_2) and back (polymer) side illumination in Figure 3 (a) shows that without additional treatments, the spin coated polymer does not penetrate into the thick (600 nm) porous TiO_2 layer, while Figure 3(b) shows that polymer penetration is achieved by surface and heat treatment.

Figure 3(b) shows the transient absorption signals of a multilayer sample containing a 600 nm porous TiO_2 layer which was treated with titanium isopropoxide solution before spin coating the polymer and was annealed at 300°C to melt the polymer into the pores. The $Ti(iPr)_4$ surface treatment is intended to remove surface water and enhance the adhesion of the polymer to the TiO_2 surface. Figure 3(a) shows transient absorption signals of an untreated sample. In both cases the transient optical signal is measured for illumination from the back (polymer side) and front sides. Comparison of these signals reveals the extent of polymer penetration into the film. In the case of the untreated sample, the lower signal with different kinetics for back side than front side illumination indicates that less light reaches the charge separating interface for back side illumination. This is attributed to poor polymer penetration into

the porous film, leaving a layer of polymer on the back side of the film which attenuates the light reaching the TiO_2/polymer interface. For the treated sample, the signals for back and front side illumination are similar, indicating effective penetration of polymer into the highly structured TiO_2. The charge separation yield is higher, suggesting better interfacial contact. (We estimate the charge separation yield as close to unity from the polaron extinction coefficient). However, the faster decay of the signal for the treated sample indicates that recombination is accelerated by the treatments, with the polaron half life reducing from ~10 ms to ~100 µs. Nevertheless the lower value still compares favourably with values reported for polymer-fullerene blends (1-100µs)[30] and solid dye sensitised solar cells[31-32].

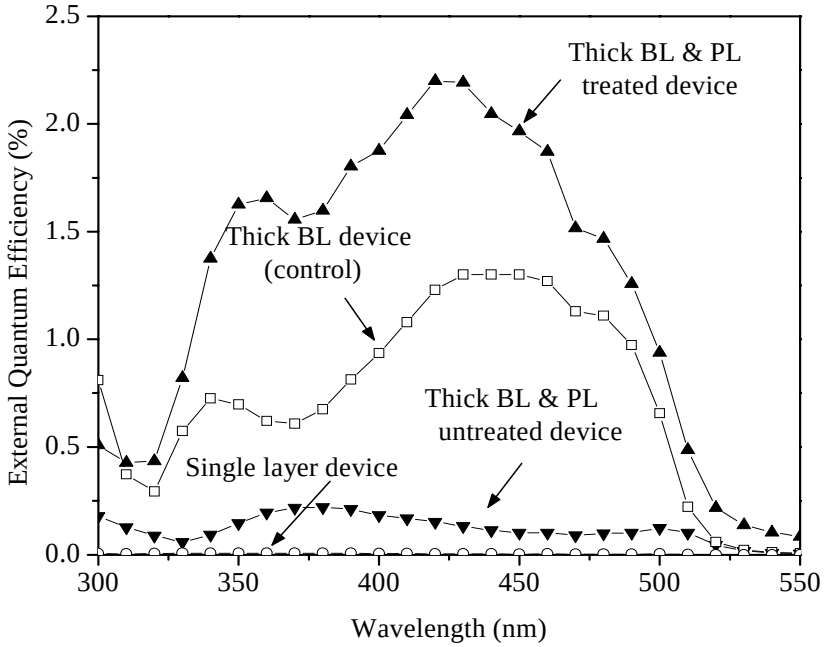

Figure 4. Quantum efficiency spectra of single layer (ITO/F8T2(100 nm)/Au) device and treated and untreated (ITO/HBL(100 nm)/Porous TiO_2(600 nm)/F8T2(200 nm)/Au) devices compared with bi-layer (ITO/HBL(100 nm)/F8T2(100 nm)/Au device.

Figure 4 compares the quantum efficiency spectra of single layer and untreated and treated multilayer devices with bi-layer devices. The quantum efficiency of the single layer device is greatly, well over 200 times, improved by addition of the dense TiO_2 layer. For the single layer device, the peak quantum efficiency is less than 0.01%, while the bi-layer device, ITO/HBL(100nm)/F8T2(100nm)/Au, is 1.3 % at the absorption maximum of the polymer. This is attributed to the action of the dense TiO_2 as a hole blocking layer, preventing short circuits. Introduction of a thick porous TiO_2 layer between the HBL and polymer layer, reduces the quantum efficiency again. This may be due to the lower charge separation yield and the increased series resistance of the additional TiO_2 layer. However, improved QE is achieved after the surface and heat treatment steps. This is consistent with the charge separation studies described above. Thus, the treatments are needed for polymer penetration into the pores of the TiO_2 in thick layer devices. In the case of thin devices (ITO/HBL(50nm)/PorousTiO_2(100nm)/F8T2(75nm)), surface and annealing treatments were not necessary to assist polymer penetration into thin (<=100nm) porous TiO_2 films. Transient absorption studies (see section 3.4) confirm that polymer penetration is achieved in to thin porous films without additional process steps.

3.3 Effect of thickness and interface morphology

The effect of layer thickness and morphology on device performance was examined. Quantum efficiency spectra for different device structures are compared in Figure 5. The details of the corresponding devices are given in Table 1. We compare the peak QE of the devices in the same table. All devices were contacted with Au contacts and illuminated through the ITO.

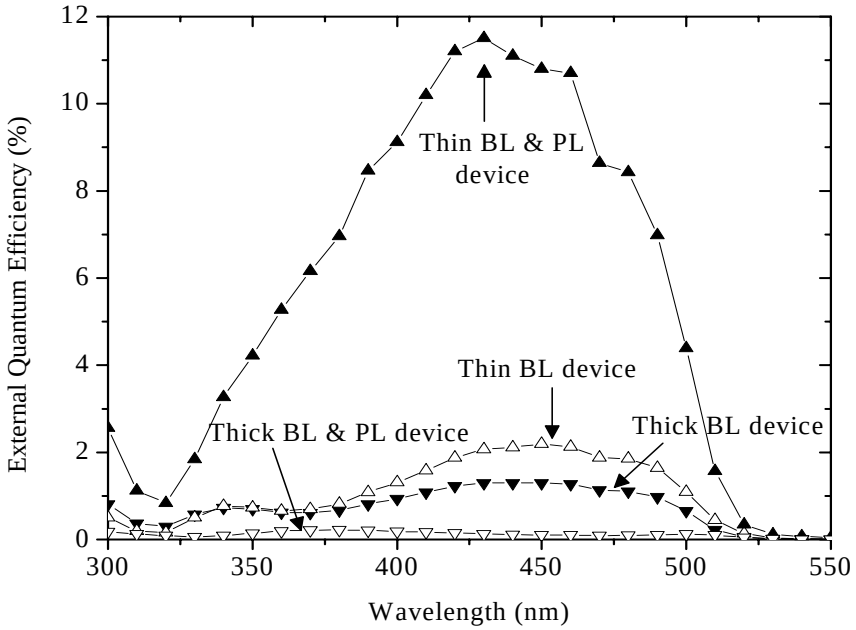

Figure 5. Quantum efficiency spectra of ITO/TiO_2/F8T2/Au devices with different TiO_2 and polymer layer thickness and different surface morphology. Details of the structures and layer thickness of the corresponding devices are given in table 1.

Table I: Layer thicknesses and peak quantum efficiency of devices presented in Figure 4 and 5.

Devices	**HBL (nm)**	**Porous TiO_2 Layer (PL) (nm)**	**Polymer Layer (nm)**	**Peak QE (%)**
Thick BL	100	-	100	**1.3**
Thick BL & PL, untreated	100	600	200	**0.2**
Thick BL & PL, treated	100	600	200	**2.2**
Thin BL	50	-	50	**2.2**
Thin BL & PL	50	100	75	**11.5**

The comparison shows that the external quantum efficiency of TiO_2/F8T2 structure is highly dependent on both layer thickness and interface morphology. Simple bi-layer devices with thin TiO_2 perform better than thicker devices, due to reduced series resistance. Although introduction of a thick porous layer into a thick bi-layer device reduces the quantum efficiency, introducing a thin porous layer into a thin bi-layer device increases the quantum efficiency by a factor of five. Thus, the thin layer device with increased interface morphology offers the best peak quantum efficiency, of 11.5 % at 440 nm, among the fabricated devices. The device produced a monochromatic power conversion efficiency of 1 % at 440 nm. Annealing and surface treatments were not necessary to achieve pore penetration in such thin layer structures.

3.4 Effect of dip-treatment

The effect of dip-coating the TiO_2 with polymer before spin coating the polymer was examined. To introduce a dip coated layer between the porous TiO_2 electrode and the spin coated polymer layer, the porous TiO_2 electrodes were immersed in a solution of F8T2 in toluene (2 mg/ml) at 50 ^{0}C for several hours prior to spin coating the polymer.

Figure 6 compares the recombination kinetics in ITO/HBL/Porous TiO_2(100nm)/F8T2 structures with dip-coated F8T2, spin-coated F8T2 layers and both. The estimated thickness of the dip coated polymer layer via optical absorption measurement is about 0.3 nm. Since the size of transient absorption signal for the structure which is dipped

only (Figure 6(a)) is similar to the signal for structure which is both dip- and spin coated; we infer the charge separation occurs very close to the TiO_2 nanocrystal-polymer interface. Similar kinetics for back and front side illumination in both samples indicates that very effective polymer penetration is achieved by dip coating.

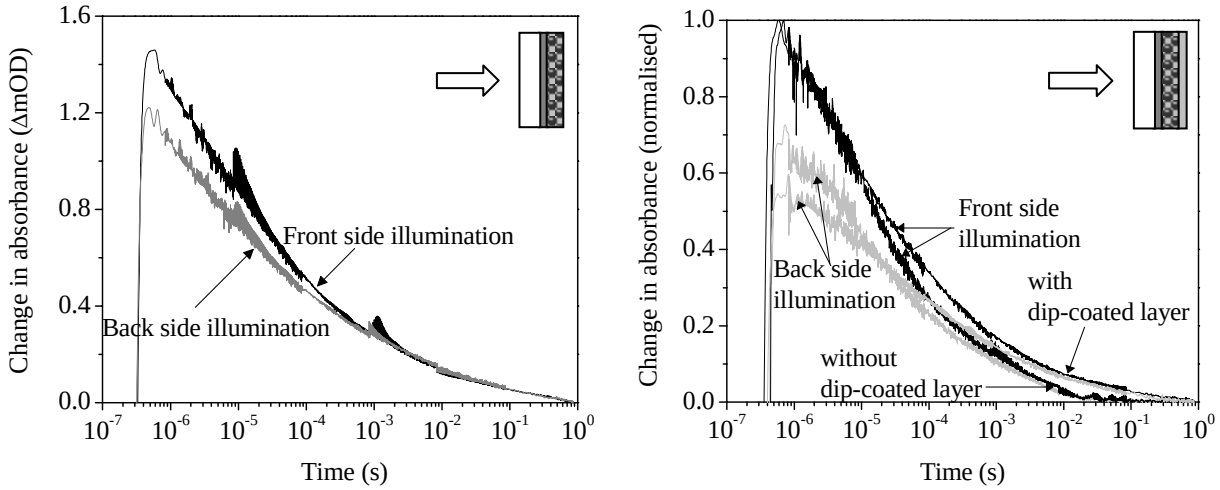

Figure 6. Transient absorption signals for (a) ITO/HBL/Porous TiO_2(100 nm)/F8T2^d and (b) ITO/HBL/Porous TiO_2(100 nm)/F8T2^d/F8T2^s(75 nm) and ITO/HBL/Porous TiO_2(100 nm)/F8T2^s(75 nm) where superscript d indicates 'dip coated' and s, is 'spin coated'. The insert shows the sample structures. The transient absorption due to the positive polaron state of the F8T2 polymer at 720nm following laser pulse excitation at 500nm, at an excitation density of 30 μJ/pulse/cm^2. The decay is assigned to recombination between electrons in TiO_2 and F8T2$^+$ polarons. Black curves represent transient absorption kinetics for front side illumination, while grey curves represent back side illumination.

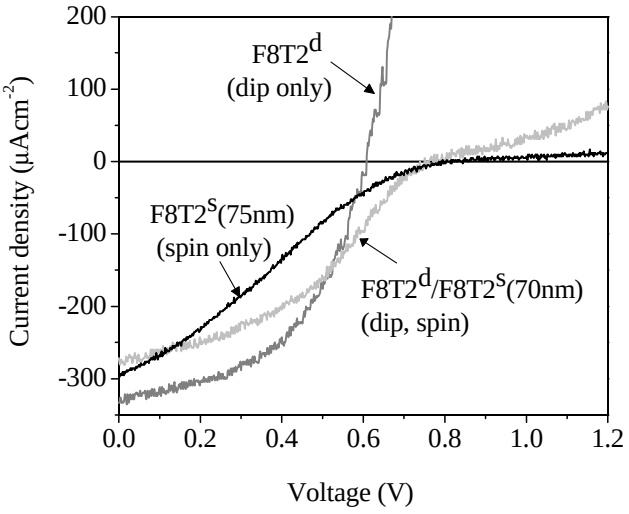

Figure 7. J-V characteristic of ITO/HBL/Porous TiO_2(100 nm)/F8T2/Au devices with different F8T2 layer thicknesses under under AM1.5 illumination (100 mWcm^{-2}).

Figure 6(b) shows the charge separation kinetics of structures ITO/HBL(50 nm)/Porous TiO_2(100 nm)/F8T2^s (75 nm) with and without a dip coated layer. Lower signal observed for back side than front side illumination indicates incomplete polymer penetration. However, the shape of kinetics for front and back side illumination is similar for both

samples and indicating that polymer penetration is achieved by either spin coating or by using a dip coating step in thin structures. Figure 6 (b) further indicates that the recombination kinetics are slightly slower when the dip coated layer is introduced.

The effect of the dip coated layer on photovoltaic performance is examined using devices based on similar structures. J-V characteristics of the devices under solar simulator illumination of intensity 100 $mWcm^{-2}$ are shown in Figure 7. The device with spin coated polymer only showed V_{oc} of 0.8V and J_{sc} of 300 μA cm^{-2} under simulated AM 1.5 radiation. However, the current falls off before reaching V_{oc}, leading to a point of inflection or 'kink' in the I-V curve and low fill factor (0.24). Similar shapes of I-V curves have been observed elsewhere for polymer/TiO_2 structures[15,19,21] and molecular film solar cells[9]. We will discuss the origin of this effect by varying light intensity, wavelength, and polymer in the next section.

The fill factor of the device is increased from 0.24 to 0.40 and the overall device performance is increased by 50 % when a dip coated layer is introduced. The device with only a dip coated layer also produced a better short circuit current density of 330μAcm^{-2} and fill factor of 0.50 but a reduced open circuit voltage of 0.61 V. Comparison of the devices with a dip coated layer and both dip- and spin coated layer suggests that part of the spin coated layer on Au side in later device acts as an optical filter due to the small exciton diffusion length (~less than 5 nm[29]) of the F8T2 polymer. Generally only excitons which are generated within a diffusion length of the interface are able to contribute to the current[33]. The others recombine before they reach an interface. Decreasing polymer layer thickness may reduce the recombination deep within polymer layer. Although decreasing thickness of the photoactive polymer leads to reduced absorption and exciton generation, it is generally only excitons generated within a few tens of nm of the interface that contribute to the current and rest of it acts as an optical filter and increase the series resistance to the device. In ref. [29], we show that the de-graded J-V characteristic steadily improves with decreasing polymer thickness. The model described in ref. [34] explains this result.

3.5 Effect of interfacial step

In this section we will examine the kink in J-V curve by varying the light intensity and wavelength and by using an alternative polymer. Figure 8 shows that the effect becomes more pronounced under increasing light intensity. This shows that it is not due to an effect of charge trapping in the system, since such effects would become less important, not more, at higher illumination levels. Varying the illumination wavelength while keeping the same photocurrent density allows us to study the effect of photogeneration profile, to see if the effect is related to a diffusive driving force for photocurrent generation. Varying the wavelength from 470 nm to 510 nm, which changes the absorption coefficient from 3×10^5 to 1×10^5 cm^{-1}, had no observable effect on the shape of the curve (data not shown).

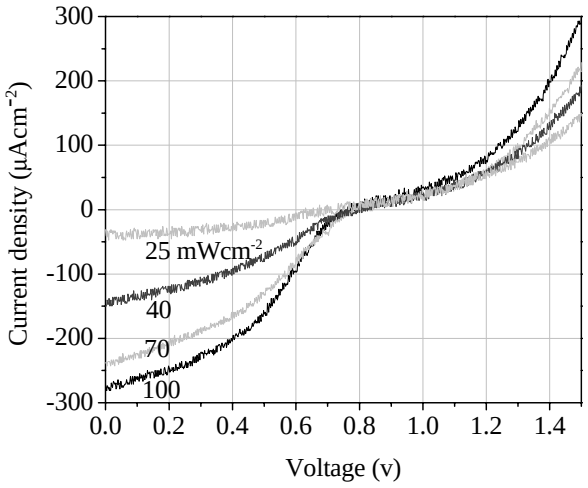

Figure 8. J-V characteristics of ITO/HBL(50 nm)/Porous TiO_2(100 nm)/F8T2^d/F8T2^s(70nm)/Au devices under simulated sunlight at different intensities.

To study whether the energy step at the polymer-metal interface might be responsible for the kink in the J-V characteristics, we varied the energy step by using alternative polymers and contact metals. In Figure 9 (a) light (monochromatic) and (b) dark J-V characteristics are presented for two bi-layer devices, one containing 50 nm of F8T2 polymer (ionisation potential 5.5 eV) and the other PFB polymer (ionisation potential 5.1 eV). In the case of the

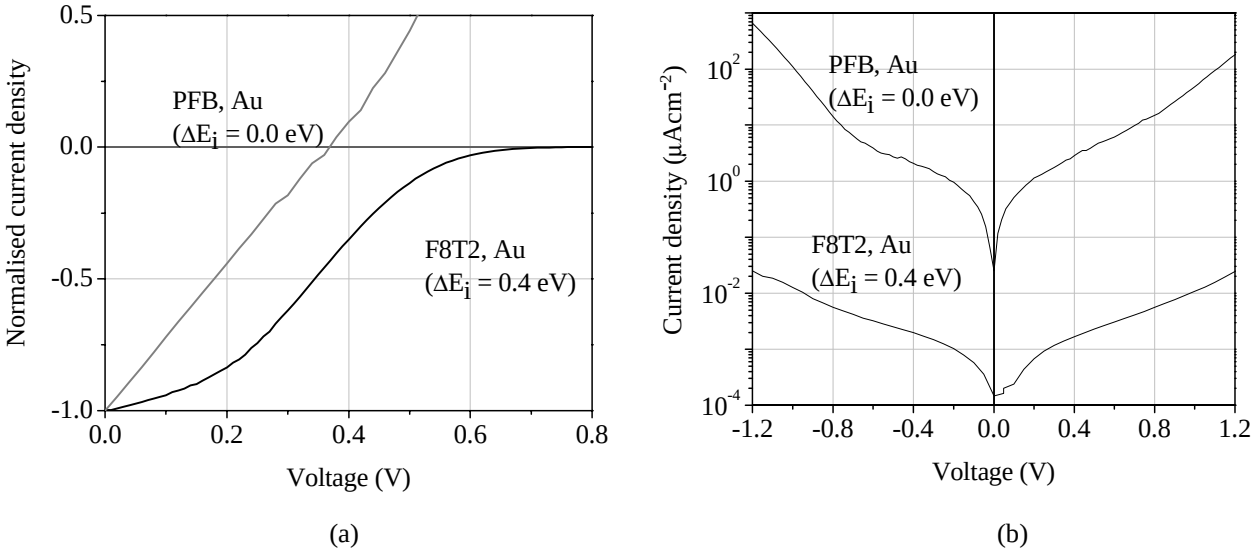

(a) (b)

Figure 9. J-V characteristic of ITO/HBL/F8T2/Au and ITO/HBL/PFB/Au bi-layer devices (a) under monochromatic illumination and (b) in dark.

PFB polymer, the dark current is higher, as expected from the much better match of metal work function to the HOMO level of the polymer. The kink has disappeared and the fill factor is better than for the F8T2 device, although the overall efficiency is lower. The lower V_{oc} for the PFB than the F8T2 device is consistent with easier charge transfer at the Au-polymer contact. Additional studies on ITO/TiO_2 /F8T2/Pt devices again showed the increase in dark current and improvement in fill factor, confirming that the effect is indeed due to the polymer-metal interface and not to the polymer-TiO_2 interface[29]. The work function of Pt (5.6 eV) is well matched to the HOMO level of F8T2 (5.5 eV). An explanation for the origin of the kink in the I-V curve is given elsewhere[34].

4. CONCLUSIONS

In summary, we have studied charge recombination and photovoltaic device performance in structures consisting of a fluorene-bithiophene co-polymer and nanocrystalline TiO_2. Efficient photoinduced charge transfer is observed using a TiO_2 film of high interfacial area while charge recombination between the hole in the polymer and the electron in the TiO_2 is slow (~100 μs-10ms). Polymer penetration into the pores of thin (<150 nm) porous TiO_2 films is achieved by spin coating without any additional processing steps, while additional surface treatment of TiO_2 and melting of the polymer was needed to achieve polymer penetration into pores for thicker TiO_2 films. Comparison of different (Al and Au) top contacts confirms that electrons travel more easily in the TiO_2 and holes in the polymer. High work function top contacts are necessary for efficient photocurrent collection and our results suggest that the energy step between HOMO of the polymer and the work function of the top contact should be small for good fill factors. Inserting a thin porous TiO_2 layer into a thin bi-layer device increases the QE by a factor of five and the device produced a short circuit current density of 300 μAcm^{-2}, a fill factor of 0.24 and an open circuit voltage of 0.8 V under AM 1.5 illumination. The fill factor is increased from 0.24 to 0.40 by introducing an additional dip coating layer and overall power conversion efficiency is increased by about 50 %.

ACKNOWLEDGEMENTS

We are grateful to The Dow Chemical Company for providing the poly(9,9-dioctylfluorene-co-bithiophene) (F8T2) and poly(9,9-dioctylfluorene-*co*-bis-*N*,*N*'-(4-butyl phenyl)-bis-*N*,*N*'-phenyl-1,4-phenylenediamine) (PFB) samples and to Alex Green and Emilio Palomares for the preparation of the TiO_2 paste. PR acknowledges the Association of Commonwealth Universities for a Commonwealth Scholarship. JN acknowledges the EPSRC for the award of an Advanced Research Fellowship.

REFERENCES

[1] M. Grätzel, *"Photo-electrochemical cells"*, Nature **414**, 338-344, 2001.

[2] J. J. M. Halls and R. H. Friend, *Clean Electricity from Photovoltaics*, 377–445, Imperial College Press, London, 2001.

[3] C. J. Brabec, N. S. Sariciftci, and J. C. Hummelen, *"Plastic Solar Cells"*, Adv. Func. Mat. **11**, 15-26, 2001.

[4] J.-M.Nunzi, *"Organic photovoltaic materials and devices"*, C. R. Physique **3**, 523-242, 2002.

[5] J. Nelson, *"Organic photovoltaic films"*, Materials Today **5**, 20-27 (2002).

[6] M.K.Nazeeruddin, A. Kay, I. Rodicio, R. Humphry-Baker, E. Muller, P. Liska, N. Vlachopoulos, and M. Gratzel, *"Conversion of light to electricity by cis-x2bis(2,2'-bipyridyl-4,4'-dicarboxylate) ruthenium(ii) charge-transfer sensitizers (x = cl-, br-, i-, cn-, and scn-) on nanocrystalline TiO_2 electrodes"*, J. Am. Chem. Soc. **115**, 6382-6390, 1993.

[7] W. U. Huynh, J. J. Dittmer, and A. P. Alivisatos, *"Hybrid Nanorod-Polymer Solar Cells"*, Science **295**, 2425-2427, 2002.

[8] U. Bach, D. Lupo, P. Comte, J. E. Moser, F. Weissortel, J. Salbeck, H. Spreitzer, and M. Gratzel, *"Solid-state dye-sensitized mesoporous TiO_2 solar cells with high photon-to-electron conversion efficiencies"* Nature **395**, 583-585, 1998.

[9] P. Peumans and S. R. Forrest, Appl. Phys. Lett. **79**, *"Very-high-efficiency double-heterostructure copper phthalocyanine/C60 photovoltaic cells*", 126-128, 2001.

[10] J. Krüger, R. Plass, and M. Grätzel, *"Improvement of the photovoltaic performance of solid-state dye-sensitized device by silver complexation of the sensitizer cis-bis(4,4-dicarboxy-2,2bipyridine)-bis(isothiocyanato) ruthenium(II)"*, Appl. Phys. Lett. **81**, 367-369, 2002.

[11] C. J. Brabec, S. E. Shaheen, C. Winder, N. S. Sariciftci, and P. Denk, *"Effect of LiF/metal electrodes on the performance of plastic solar cells"*, Appl. Phys. Lett. **80**, 1288-1290, 2002.

[12] N. C. Greenham, X. Peng, and A. P. Alivisatos, *"Charge separation and transport in conjugated-polymer/semiconductor-nanocrystal composites studied by photoluminescence quenching and photoconductivity"*, Phys. Rev. B **54**, 17628-17637, 1996.

[13] T. J. Savenije, J. M. Warman, and A. Goossens, *"Visible light sensitisation of titanium dioxide using a phenylene vinylene polymer"*, Chem. Phys. Lett. **287**, 148-153, 1998.

[14] N. A. Anderson, E. Hao, X. Ai, G. Hastings, and T. Lian, *"Ultrafast and long-lived photoinduced charge separation in MEH-PPV/nanoporous semiconductor thin film composites"*, Chem. Phys. Lett. **347**, 304-310, 2001.

[15] A. J. Breeze, Z. Schlesinger, and S. A. Carter, *"Charge transport in TiO_2/MEH-PPV polymer photovoltaics"*, Phys. Rev. B **64**, 1252051-1252059, 2001.

[16] Q. Fan, B. McQuillin, D. D. C. Bradley, S. Whitelegg, A. B. Seddon, *"A solid state solar cell using sol-gel processed material and a polymer"*, Chem. Phys. Lett. **347**, 325-330, 2001.

[17] M. Y. Song, J. K. Kim, K. J. Kim, and D. Y. Kim, *"Photovoltaic characteristics of TiO_2/conjugated polymer junctions"*, Synth. Met. **137**, 1387, 2003.

[18] A. C. Arango, S. A. Carter, and P. J. Brock, *"Charge transfer in photovoltaics consisting of interpenetrating networks of conjugated polymer and TiO_2 nanoparticles"*, Appl. Phys. Lett. **74**, 1698-1700, 1999.

[19] A. C. Arango, L. R. Johnson, V. N. Bliznyuk, Z. Sclesinger, S. A. Carter and H. H. Horhold, *"Efficient Titanium Oxide/conjugated polymer photovoltaics for solar energy conversion"*, Adv. Mater. **12,** 1689, 2000.

[20] P. A. V. Hal, M. M. Wienk, J. M. Kroon, W. J. H. V. Gennip, P. Jonkheijm, and R. A. J. Janssen, *"Photoinduced Electron Transfer and Photovoltaic response of a MDMO PPV:TiO_2 Bulk-Heterojunction"*, Adv. Mater. **15**, 118-121, 2003.

[21] M. Kaneko, K. Takayama, S. S. Pandey, W. Takashima, T. Endo, M. Rikukawa, and K. Kaneto, "*Photovoltaic cell using high mobility poly (alkylthiophene)s and TiO_2"*, Synth. Met. **121**, 1537-1538, 2001.

[22] D. Gebeyehu, C. J. Brabec, F. Padinger, T. Fromherz, S. Spiekermann, N. Vlachopoulos, F. Kienberger, H. Schindler, and N. S. Sariciftci, "*Solid state dye-sensitised TiO_2 solar cells with poly(3-octylthiophene) as hole transport layer*, Synth. Met. **121**, 1549-1550, 2001.

[23] C. D. Grant, A. M. Schwartzberg, G. P. Smestad, J. Kowalik, L. M. Tolbert, and J. Z. Zhang, "*Characterization of nanocrystalline and thin film TiO_2 solar cells with poly (3-undecyl-2,2'-bithiophene) as a sensitizer and hole conductor"*, J. Elec. Anal. Chem. **522**, 40-48, 2002.

[24] H. Sirringhaus, R. J. Wilson, R. H. Friend, M. Inbasekaran, W. Wu, E. P. Woo, M. Grell, and D. D. C. Bradley, "*Mobility enhancement in conjugated polymer field-effect transistors through chain alignment in a liquid-crystalline phase"*, App. Phys. Lett. **77**, 406-408, 2000.

[25] M. Grell, M. Redecker, K. S. Whitehead, D. D. C. Bradley, M. Inbasekaran, E. P. Woo, "*Monodomain alignment of thermotropic fluorene copolymers"*, Liquid Crystals **26**, 1403-1407, 1999.

[26] R. L. Willis, C. Olson, B. O'Regan, T. Lutz, J. Nelson, and J. R. Durrant, "*Electron dynamics in nanocrystalline ZnO and TiO_2 Films Probed by Potential Step Chronoamperometry and Transient Absorption Spectroscopy"*, J. Phys. Chem. B **106,** 7605-7613, 2002.

[27] L. Kavan and M. Grätzel, Electrochimica Acta **40**, "*Highly efficient semiconducting TiO_2 photoelectrodes prepared by aerosol pyrolysis"*, 643-652, 1995.

[28] S. A. Haque, Y. Tachibana, D. R. Klug, and J. R. Durrant, "*Charge Recombination Kinetics in Dye-Sensitized Nanocrystalline Titanium Dioxide Films under Externally Applied Bias"*, J. Phys. Chem. B **102,** 1745-1749, 1998.

[29] P. Ravirajan, S. A. Haque, D. Poplavskyy, J. R. Durrant, D. D. C. Bradley, and J. Nelson, "*Hybrid nanocrystalline TiO_2 solar cells with a fluorene-thiophene copolymer as sensitizer and hole-conductor"*, J. Appl. Phys. (submitted).

[30] I. Montanari, A. F. Nogueira, J. Nelson, J. R. Durrant, C. Winder, M. A.Loi, N. S. Sariciftci, and C. Brabec , "*Transient optical studies of charge recombination dynamics in a polymer/fullerene composite at room temperature"*, Appl. Phys. Lett. **81**, 3001, 2002.

[31] S. A. Haque, Y. Tachibana, R. L. Willis, J. E. Moser, M. Grätzel, D. R. Klug, and J. R. Durrant, "*Parameters Influencing Charge Recombination Kinetics in Dye-Sensitized Nanocrystalline Titanium Dioxide Films"*, J. Phys. Chem. B **104,** 538-547, 2000.

[32] J. Krüger, R. Plass, L. Cevey, M. Piccirelli, U. Bach, and M. Grätzel, "*High efficiency solid-state photovoltaic device due to inhibition of interface charge recombination"*, Appl. Phys. Lett. **79**, 2085-2087, 2001.

[33] K. Petritsch and R. H. Friend, "*Ultrathin Organic Photovoltaic Devices"*, Synth. Met. **102**, 976, 1999.

[34] J. Nelson, J. Kirkpatrick and P. Ravirajan, "*Factors limiting the efficiency of molecular photovoltaic devices"*, Phys. Rev. B. (submitted).